Assessing the temporal stability of spatial patterns of soil apparent electrical conductivity using geophysical methods

Sunshine A. De Caires*, Mark N. Wuddivira, and Isaac Bekele

Department of Food Production, University of West Indies, St. Augustine, Trinidad and Tobago, West Indies

A b s t r a c t. Cocoa remains in the same field for decades, resulting in plantations dominated with aging trees growing on variable and depleted soils. We determined the spatio-temporal variability of key soil properties in a (5.81 ha) field from the International Cocoa Genebank, Trinidad using geophysical methods. Multi-year (2008-2009) measurements of apparent electrical conductivity at 0-0.75 m (shallow) and 0.75-1.5 m (deep) were conducted. Apparent electrical conductivity at deep and shallow gave the strongest linear correlation with clay-silt content (R = 0.67 and R = 0.78, respectively) and soil solution electrical conductivity (R = 0.76 and R = 0.60, respectively). Spearman rank correlation coefficients ranged between 0.89-0.97 and 0.81-0.95 for apparent electrical conductivity at deep and shallow, respectively, signifying a strong linear dependence between measurement days. Thus, in the humid tropics, cocoa fields with thick organic litter layer and relatively dense understory cover, experience minimal fluctuations in transient properties of soil water and temperature at the topsoil resulting in similarly stable apparent electrical conductivity at shallow and deep. Therefore, apparent electrical conductivity at shallow, which covers the depth where cocoa feeder roots concentrate, can be used as a fertility indicator and to develop soil zones for efficient application of inputs and management of cocoa fields.

K e y w o r d s: apparent electrical conductivity, electromagnetic-induction, humid tropics, spatial patterns, temporal stability

INTRODUCTION

Cocoa (*Theobroma cacao* L.) plantations have a problem of within-field yield variability which may originate form spatial variation is soil properties (Eneje *et al*., 2012; Obalum *et al*., 2013). Once established, cacao remains in the same field for decades, therefore cocoa fields are dominated with aging trees growing on variable and depleted soils (Snoeck *et al*., 2010). In Trinidad and Tobago like many cocoa producing countries, increase in cocoa production is mainly due to expansion of existing farms or creation of new farms rather than increase in yield per unit area (Gockowski, 2007; Snoeck *et al.*, 2010). While technological approaches to address within-field variability have resulted in stupendous increase in yield per unit area in the production of other crops, cocoa production still relies on inefficient and outdated traditional production and management methods that do not take into account within-field soil variability. Uniform management of large cocoa plantations have resulted in less than optimum yields and economic returns due to nutrient deficiencies as well as excessive fertilizer application that may potentially reduce environmental quality (Schumann *et al*., 2003). Therefore, there is an emerging need for cocoa producers to increase input efficiency, improve the economic margins of crop production, and reduce environmental risks, which can be achieved if site-specific precision management of plantations is employed.

Precision agriculture seeks to develop agronomic strategies to manage spatially variable fields more efficiently by developing management zones or subregions of a field with homogeneous yield-limiting factors (Doerge, 1999; Rossi *et al*., 2013). This holistic system approach depends on understanding and accurately identifying the underlying factors responsible for variation in crop yield (Mann *et al*., 2011). Since soils and their properties play a distinctive role in determining the productivity of agricultural fields, once a sound understanding of the within-field variability of soil physicochemical properties in cocoa plantations

---

*Corresponding author e-mail: sunshine.decaires@live.com

is established, management zones can be developed and recommendations made for varying inputs. Apparent soil electrical conductivity (EC$_a$) has shown great potential for identifying yield limiting soil properties and used successfully to develop management zones (Mann *et al*., 2011; Moral *et al*., 2010).

Electromagnetic induction (EMI) sensors such as DUALEM-1S EC meter employ geophysical imaging techniques to rapidly, non-invasively measure spatial variations of soil ECa (Atwell *et al*., 2013; Bréchet *et al*., 2012; Rossi *et al*., 2013; Wuddivira *et al*., 2012). Apparent soil electrical conductivity correlates with various physicochemical soil properties such as salinity (Rhoades *et al*., 1999), clay content (Triantafilis and Lesch, 2005; Wuddivira *et al*., 2012), water content (Haimelin, 2008) and carbon content (Martinez *et al*., 2009). Recently, Atwell *et al*. (2013) and Bréchet *et al*. (2012) showed that under humid tropical conditions, variation in ECa was influenced by temporal changes in soil moisture content, spatial variation of clay-silt mineral content, soil solution electrical conductivity (ECe) and soil water repellency. Thus, EMI sensors provide the prospect of cost effectively collecting dense spatial data, combining sufficient scale triplet of spacing, extent and support to capture small and large scale variability of soil properties (Atwell *et al*., 2013).

Electromagnetic induction measurements using DUALEM-1S EC meter are sensitive to the upper 0-0.75 m for EC$_a$$_s$ and the lower 0.75-1.5 m for EC$_a$$_d$, making it especially beneficial to management zone development in cocoa plantations, since cocoa trees obtain moisture and nutrients from a mat of lateral roots which lie in the top 0.2 m (Wood and Lass, 1985). Although, researchers have investigated the spatio-temporal stability of ECa in temperate regions (King *et al*., 2001; Nehmdahl and Greve, 2001), there has been limited research on tropical soils (Robinson *et al*., 2009). Even so, there are no reports of studies on cocoa soils using geophysical imaging to assess the temporal stability of spatial patterns of ECa to develop management zones. Temporal stability is important in order to make mana- gerial agricultural decisions based on spatial variability. King *et al*. (2001) and Nehmdahl and Greve (2001) both noted that in order to characterize ECa, multiple surveys yielding similar patterns over time, regardless of external factors, should be undertaken. This is of vital importance if zones developed based on ECa patterns are to be used to manage the field for multiple years (Farahani and Buchleiter, 2004), as would be the case for cocoa plantations.

Farahani and Buchleiter (2004) compared the stability of EC$_a$$_s$ and EC$_a$$_d$ in three irrigated sandy fields in eastern Colorado and found EC$_a$$_d$ to be more temporally stable than the corresponding EC$_a$$_s$. This was expected as the top soil layer is subjected to more fluctuation in transient properties such as water content (WC) and temperature. The magnitude of fluctuation depends on climatic factors (rainfall and temperature) and the type of crop cover. Fluctuations in the top

soil layer will therefore be more pronounced in semi-arid regions and in fields cultivated to annual crops resulting in more temporally unstable EC$_a$$_s$ than in the humid tropics in fields grown to permanent tree crops. We hypothesize that due to the perennial nature of cocoa trees, thick organic litter and understory cover coupled with little fluctuation in soil water and temperature in the humid tropics, EC$_a$$_s$ will be as temporally stable as EC$_a$$_d$. The objectives of our study were to:
- investigate the temporal stability of spatial patterns of apparent soil electrical conductivity,
- determine which soil properties contribute to electromagnetic induction signals in a humid tropical cocoa field.

MATERIALS AND METHODS

The study was conducted at the International Cocoa Genebank, Trinidad (ICG, T), 10° 34' 39" N, 61° 18' 0" W (Fig. 1a). The ICG, T consists of 33 ha of land divided into five fields (Fig. 1b). Cocoa plants were established between 1986 and 1990. Permanent shade was provided by Erythina spp. and temporary shade by the original 'old' cocoa trees and non-commercial bananas (Musa acuminate). Our study was conducted on a 5.81 ha field (blocks 6A and 6B) that is prone to seasonal flooding by the Caroni River, which may redistribute soil particles, alter the absolute magnitude of ECa and flush any fertilizer salts from the soil that may build up from previous growing seasons. The ICG, T is subjected to humid tropical conditions, with mean annual rainfall of 2000 mm falling mainly between July and December (wet season) and a marked dry season from January to June, with less than 400 mm of rain (Granger, 1983). Average monthly temperatures range from 25.7 to 28.9°C, with an average monthly relative humidity of 81%. The ICG, T is sited on a fine silt-clay alluvium belonging to the Cunupia clay soil series (Inceptisol), which has restricted internal drainage and a flat topology.

The DUALEM-1S EC meter (Dualem, Milton, ON, Canada) described in Abdu *et al*. (2007) was used to carry out ECa mappings. The sensor was connected to an Archer Ultra Rugged-Pda field computer (Juniper Systems, Logan, UT) running HGIS software (Starpal, Ft, Collins, CO) and a GPS (REB-12R, RoyalTek, Tao Yuan, Taiwan) containing a SirfIII chipset. The sensor-field computer-GPS setup provided spatially exhaustive geo-referenced readings for EC$_a$$_s$ and EC$_a$$_d$. Using the time lapse approach (Robinson *et al*., 2009), a total of nine ECa surveys were completed between 2009 and 2010. This was done to capture multi-year spatio-temporal and seasonal changes of ECa in the cocoa field. The EMI instrument was held constantly at approximately 0.25 m above the soil surface and measurements were taken at 2 s intervals along parallel lines in both the north-south and east-west direction approximately 20 m apart (Fig. 1c).
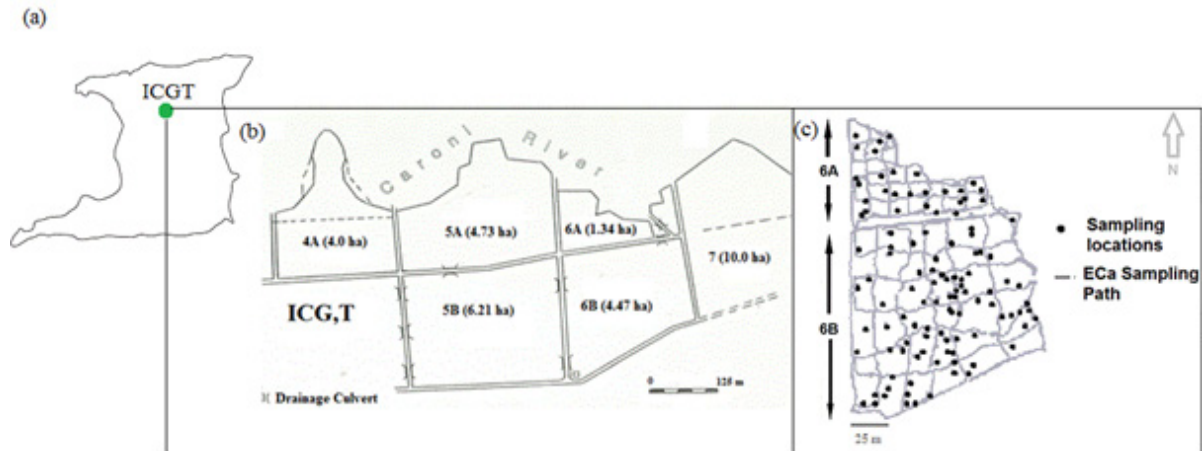
Fig. 1. (a) Map of Trinidad showing location of ICG,T (b) detailed schematic of 318 ICGT (c) apparent electrical conductivity (ECa) mapping path and sample locations.

The first EMI image was made on March 13, 2009 in the middle of the dry season. The next two images were taken towards the end of the dry season on the April 28 and May 18, 2009. Wet season surveys were performed on June 30, August 24, September 26 and November 27, 2009. The final two images were obtained during the dry season in 2010 on January 21 and June 30. Soil water content, measured with a theta probe (DeltaT Devices, Burwell, Cambridge, United Kingdom) and soil temperature, measured with a soil temperature sensor (Novel Ways Ltd, Hamilton, New Zealand) were recorded before and after the first three ECa surveys (data not shown). The soil temperature did not change from 30°C, which is consistent for tropical climates (Robinson *et al.*, 2009). Therefore, no temperature correction was needed for the data.

Data were downloaded from the field computer and subjected to QA/QC analysis to recognize and exclude data points that where obtained while the surveyor was stationary. Using a time-series view of the data, ECa values were then checked for stability and any erratic values were eliminated. As a quality control measure, inconsistent values caused by materials such as buried metal fragments, wires and pipes were identified and removed from the dataset.

The datasets were normal score transformed using S-GeMS (Remy, 2005) to prepare the data for a kriging process. The underlying assumption of kriging was that the data were normally distributed (Goovaerts, 2010). The normal score transformation was useful in transforming data with large outlying values to provide a normal distribution with a mean of 0 and a variance of 1. The normal score transform function was derived by matching the original skewed cumulative distribution function (cdf) to a standard normal cdf. Block kriging was performed on each dataset by fitting them with variograms and kriging them on a 5 x 5 m grid using VESPER (Walter *et al.*, 2001). The final ECa maps were created in S-GeMS, where the kriged data were back transformed.

Vachaud *et al.* (1985) used the differences between individual and spatial average values and Spearman rank correlation to characterize the temporal stability of parametric values. The method depends on a spatial location keeping its rank in the cdf for different sampling times (Vachaud *et al.* 1985). Since the study site was topologically flat, the supposition was that EMI mapping can capture the dominant intrinsic physical soil property through repeated mapping, by employing a temporal stability analysis technique. Ranking and/or time-lapse ECa images were used successfully by Robinson *et al.* (2009) to identify hydrologic subsurface patterns, soil texture, and water-holding capacity. The modified temporal and rank stability procedure described by Robinson *et al.* (2009) was employed in this study to determine the stability of ECa_s and ECa_d across the field.

Prior to soil sample extraction at the depth of 30 cm from 120 random sampling sites using a Dutch Cutting Auger, EMI signal (ECa) and GPS coordinates were recorded for each sites. Soil samples were transported back to the lab in Ziploc plastic bags to prevent moisture loss. Sub-samples of approximately 105 g of soil (fresh weight) were taken from each sample and analysed for gravimetric water content (θ_g) by recording dry mass after oven-drying at 105° C until constant weight was achieved. The rest of the soil was air dried, and stones and organic debris such as roots were removed from the samples. The samples were then crushed using a mortar and a pestle and passed through a 2 mm sieve. Particle size distribution, ECe and organic matter content (OM) were analysed using standard methods. pH measurements were made in 0.01 M $CaCl_2$ (soil to solution ratio 1:1) using a pH meter equipped with combination gel-filled glass electrode.

T a b l e 1. Summary statistics of deep (ECa$_d$) and shallow (ECa$_s$) apparent soil electrical conductivity

Sampling date	ECa$_d$ (mS m^{-1})					ECa$_s$ (mS m^{-1})				
	Min	Max	Mean	Std	CV	Min	Max	Mean	Std	CV
				Dry season (2009)						
March	4.50	48.62	20.84	8.43	40.43	3.10	23.50	10.66	3.44	32.30
April	1.26	86.10	17.40	8.70	49.99	1.80	13.60	6.26	2.46	39.28
May	0.65	42.34	14.84	7.46	50.27	1.69	16.70	6.02	2.25	37.35
				Wet season (2009)						
June	4.08	54.07	17.71	8.40	47.42	6.40	37.10	17.29	6.28	36.35
August	7.30	49.04	21.85	8.20	37.53	5.40	26.00	12.59	3.64	28.91
September	2.13	53.26	21.23	9.15	43.09	4.80	31.80	11.68	3.66	31.34
November	0.63	57.82	21.43	9.77	45.58	6.60	34.80	13.70	4.04	29.51
				Dry season (2010)						
January	1.74	44.95	17.12	8.09	47.22	2.30	18.90	7.36	2.61	35.44
April	1.30	26.35	10.98	6.14	55.87	1.00	9.10	3.77	1.73	45.87

RESULTS AND DISCUSSION

Summary statistics of ECa are presented in Table 1. Mean ECa values varied from 10.98 to 21.85 mS m^{-1} for ECa$_d$ and 3.77-17.29 mS m^{-1} for ECa$_s$. ECa$_s$ data ranged from 1.00 to 37.10 mS m^{-1} while ECa$_d$ ranged from 0.63 to 86.10 mS m^{-1}. June 2009 exhibited very close mean ECa$_s$ and ECa$_d$ values (Fig. 2), indicating that both depths had similar water content and temperatures on that day. Spatial variability, as quantified by coefficient of variation (CV), was generally high for all mapping events, ranging from 28.91 to 55.87%. Farahani and Buchleiter (2004) reported similar variation in CV in three irrigated sandy fields in eastern Colorado, seemingly a normal range for low salt systems. Both absolute and relative measures of variability such as standard deviations (Stdev, 1.73 to 9.77) and CV (28.91% to 55.87%) for the nine ECa$_s$ and ECa$_d$ surveys were generally high at all sites, indicating that rainfall and temperature fluxes affected the variability of ECa among survey dates. This interpretation is supported by the Spearman rank correlation coefficient (r$_s$) of ECa measurements (Table 2), where correlations are high for the wettest months surveyed. ECa$_s$ had lower means, standard deviations, and CVs than ECa$_d$ indicating less variability, which is not expected due to more exposure to climatic and anthropogenic disturbances. Moderate (0.36 < |R^2| < 0.64) to strong (|R^2| > 0 .64) positive coefficients of determination, R^2 (Fig. 3) were observed between ECa$_s$ and ECa$_d$ for all measurement days, suggesting homogeneity between shallow and deep horizons, although this is partly due to deep ECa integrating the 1.5 m soil that includes the 0.75 msoil layer represented by ECa$_s$ (Farahani and Buchleiter, 2004).

The normal score semivariograms in Fig. 4 demonstrate strong spatial structure and correlation. ECa$_d$ variograms had a slightly different structure than the ECa$_s$ models. ECa$_s$ models had slightly larger nugget, lower sill and generally shorter range values (except for April and May 2009) than corresponding ECa$_d$ models (Table 3) suggesting ECa$_s$ is less spatially continuous than ECa$_d$. The least error in the measured ECa was observed in the driest month of January 2010, which had the smallest nugget effect for both ECa$_s$ and ECa$_d$. Spherical semivariograms were fitted to both ECa$_s$ and ECa$_d$, because spherical models exhibit linear behaviour at the origin and are appropriate for representing properties with a higher level of short-range variability (Bohling, 2005). The different environmental conditions under which data was collected had only minor effects on the spatial structure of the ECa semivariograms signifying that spatial dependence isn't significantly affected by ephemeral factors, although absolute values may change.

Kriged ECa$_s$ and ECa$_d$ maps for April 2009 and April 2010 (same month, consecutive years), August 2009 (wettest survey month) and January 2010 (driest survey month) are presented in Fig. 5. Visual inspection of all maps reveals a general pattern where a zone with higher ECa approximately 50 m x 100 m was observed. For all
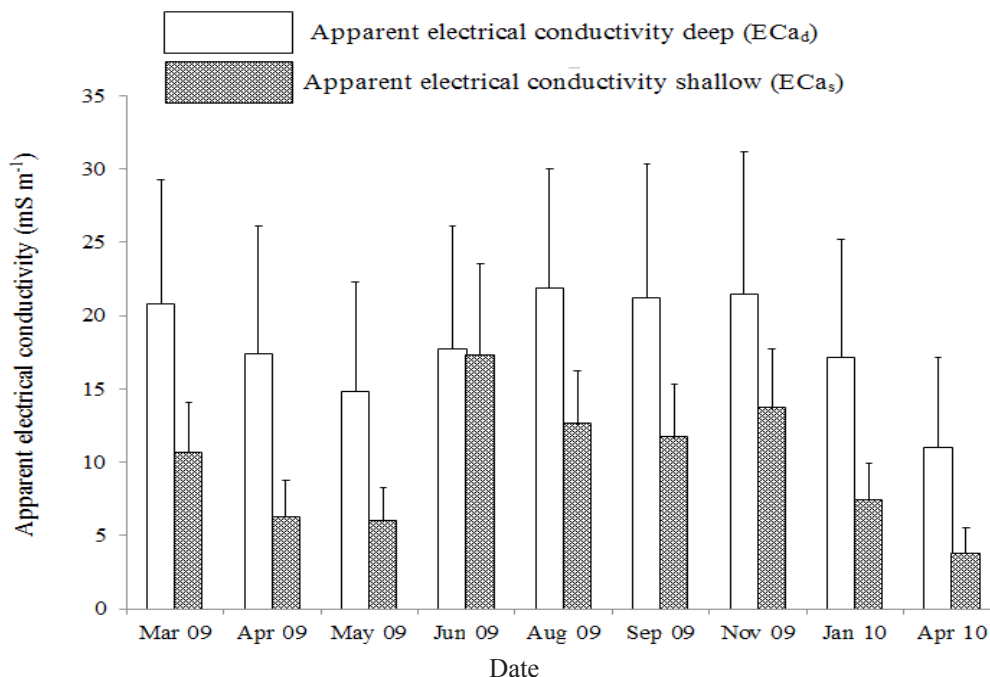
Fig. 2. Mean shallow (ECa$_s$) and deep (ECa$_d$) apparent electrical conductivity (ECa) as functions of survey dates. Error bars are standard error of the mean.

maps, the south-western end of the field had the lowest ECa values and the north-eastern side had the highest. Maps of April 2009 and April 2010 showed a lot of variability, especially at the deeper depths. Both surveys were done during a rainfall event and the pattern was interpreted to indicate the redistribution of water, changing the soil ECa as the field was mapped.

ECa$_s$ produced unimodal distributions (except June 2009) and ECa$_d$ were mildly bimodal (Fig. 6). For both ECa$_s$ and ECa$_d$, the months with the greatest cumulative precipitation exhibited histograms slightly skewed to the right while the driest months were highly skew to the right, indicating that the field should be mapped when soil water content is near field capacity. June was the only ECa$_s$ dataset to have a bimodal distribution, supporting the inference that in that month, both depths experienced similar water and temperature conditions, which would also explain the similar means for ECa$_s$ and ECa$_d$.

Data for soil physicochemical properties are presented in Table 4. The soil samples were acidic with a mean pH value of 4.4. ECe averaged 126.4 mS m^{-1} and ECa was observed to increase with depth. Thus, ECa$_s$ averaged 10.2 mS m^{-1} and ECa$_d$ averaged 17.6 mS m^{-1}. The correlation coefficients between variables is shown in Table 5. When the correlations of the soil properties and ECa were explored, both ECa$_d$ and ECa$_s$ showed strong positive linear correlation with clay-silt content (R = 0.67 and R = 0.78 respectively) and ECa$_e$ (R = 0.76 and R = 0.60, respectively). Although correlations of ECa with OM (ECa$_d$, R = 0.20;

ECa$_s$, R = 0.23) and θ_g (ECa$_d$, R = 0.28; ECa$_s$, R = 0.25) were weak at both depths, they were found to be significant at the 5% level (Table 5). Coefficient of variability (CV) for soil properties indicated significant spatial variability, suggesting the convenience of defining management zones (Moral *et al.*, 2010).

Given the varying texture and ECe across the field as indicated by the CVs, clay-silt content and ECe were expected to give the strongest correlations with the ECa signal. Although ECa is known to be strongly dependent on water content, the sampling on a single day, at a point in time, does not capture the temporal change in water content given different texture-dependent calibrations (Robinson *et al.*, 2009). Stepwise multiple regressions indicated that the most important predictors of ECa$_d$ were ECe, clay-silt content and OM, in that order, whereas the most important predictors of ECa$_s$ were clay-silt content, then ECe followed by θ_g. The regression model suggested that ECe and clay-silt content dominated the ECa$_d$ signal response accounting for 67% of its variability, whereas clay-silt content alone explained 61% of the ECa$_s$ signal response. Due to more exposure to climatic and anthropogenic disturbances, including frequent flooding, ECa$_s$ response was dominated by varying soil particle size distributions across the field. Concomitantly, the ECa$_d$ signal was most influenced by ECe suggesting that salts accumulate as soil depth increases. The ICG,T's restricted internal drainage indicates clay content increase as soil depth increases, which explains the increase in salt accumulation with depth.

T a b l e 2. Spearman rank correlation coefficients deep (ECa$_d$) and shallow (ECa$_s$) apparent soil electrical conductivity

		2009						2010	
		March	April	May	June	August	September	November	January	April
Deep apparent electrical conductivity (ECa$_d$)										
	March	1								
	April	0.945	1							
	May	0.905	0.958	1						
2009	June	0.903	0.950	0.943	1					
	August	0.935	0.956	0.949	0.906	1				
	September	0.919	0.942	0.913	0.890	0.970	1			
	November	0.916	0.923	0.908	0.888	0.972	0.970	1		
2010	January	0.914	0.939	0.938	0.927	0.957	0.932	0.954	1	
	April	0.919	0.946	0.943	0.927	0.925	0.919	0.919	0.949	1
Shallow apparent electrical conductivity (ECa$_s$)										
	March	1								
	April	0.892	1							
	May	0.860	0.920	1						
2009	June	0.805	0.856	0.830	1					
	August	0.866	0.866	0.887	0.824	1				
	September	0.855	0.857	0.873	0.834	0.951	1			
	November	0.859	0.835	0.852	0.814	0.932	0.944	1		
2010	January	0.819	0.823	0.862	0.824	0.870	0.867	0.922	1	
	April	0.780	0.867	0.886	0.853	0.811	0.844	0.826	0.904	1

Visual inspection of the kriged clay-silt content map (Fig. 7), and kriged ECa maps (Fig. 5), showed remarkably similar spatial patterns where the south-western end of the field had the lowest ECa and fine fraction values and the north-eastern side had the highest. This distribution pattern suggested that high ECa readings were consistently found in areas with finer texture, indicating that ECa can be used to interpret clay-silt content throughout the field site.

Spearman rank correlation coefficient was used to get a quantitative measure of the time stability of spatial locations between different mapping days (Table 2). The three wettest months (August, September and November 2009) had the highest Spearman's rank correlation coefficients for both ECa$_s$ and ECa$_d$. The highest occurred between August 2009 and November 2009 (ECa$_d$) and August 2009 and September 2009 (ECa$_s$) with r$_s$ values of 0.97 and 0.95, respectively. The fact that the correlations are high for the wettest months surveyed, suggest similar ECa$_s$ and ECa$_d$ responses with the increase in water content.

Figure 8 indicated locations that are consistently higher than the field ECa average and locations that are consistently lower than the field average. The lowest ranked spatial locations were 5.3 and 12.8 mS m^{-1} below the averaged mean ECa of the nine mapping events for ECa$_s$ and ECa$_d$, respectively. While the highest ranked zones were 9.6 and 30.7 mS m^{-1} above the averaged mean for ECa$_s$ and ECa$_d$, respectively. The temporal stability maps do indicate a general transition in soil texture across the field with a combined decrease in ECe and clay-silt content from the northern to the southern end of the field, as confirmed by sampled soil. The textural variation may be as a result of seasonal flooding of the study site. Beside leaching and temporary increases in soil electrical conductivity, flooding
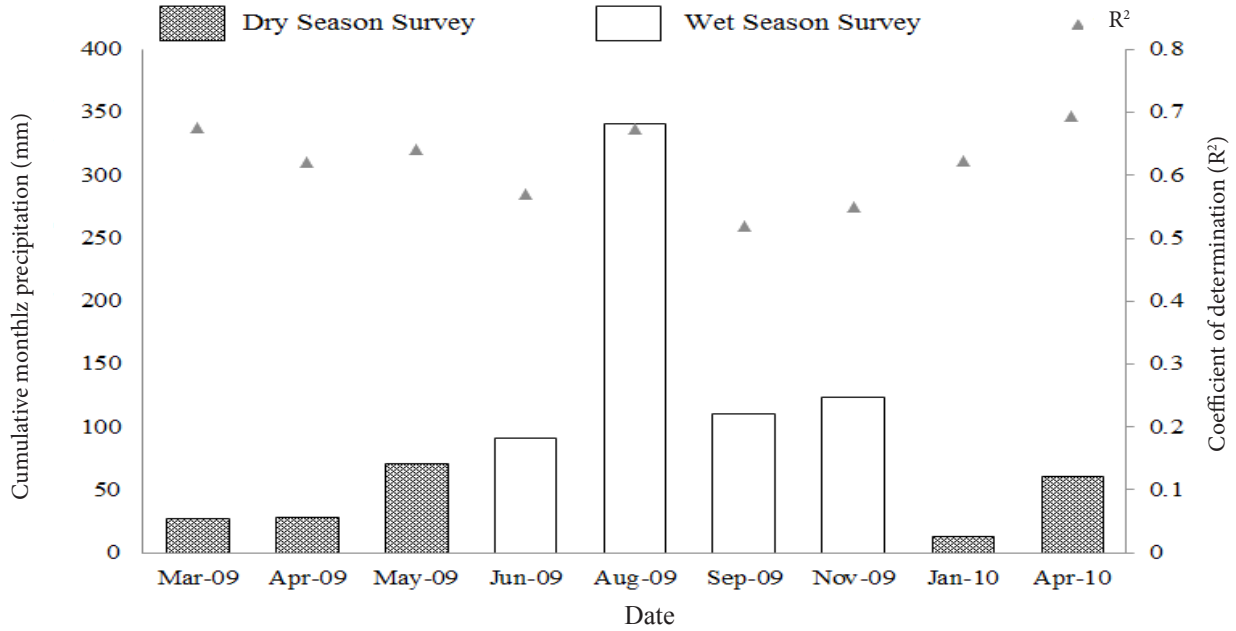
Fig. 3. Correlation coefficients of monthly shallow *vs*. deep apparent electrical conductivity values in relation to cumulative monthly precipitation.
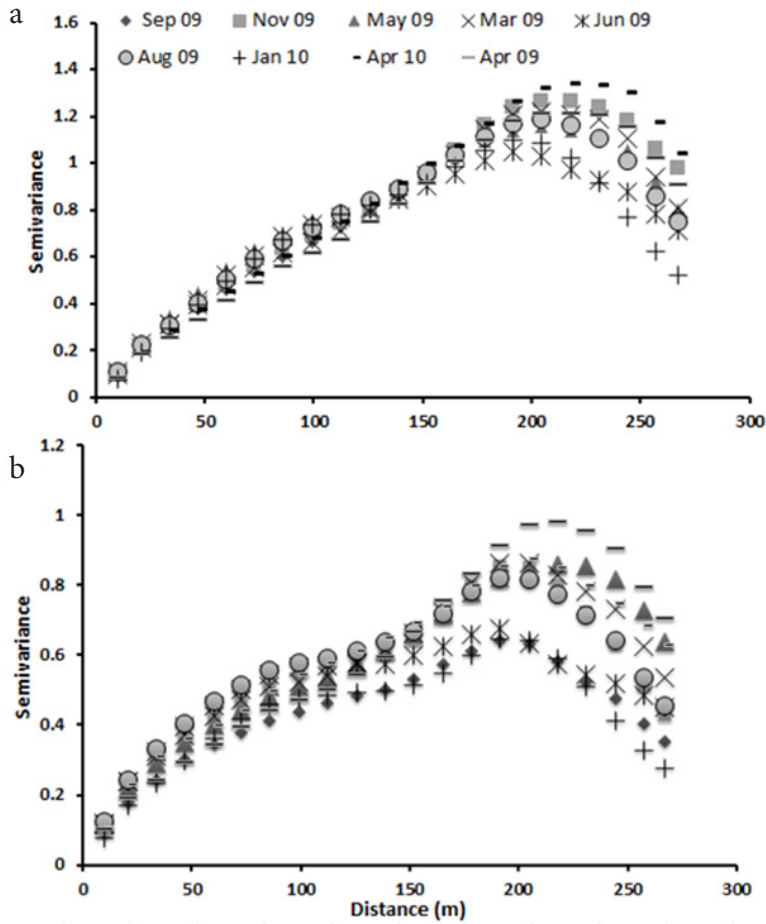

Fig. 4. Semivariograms for the kriged aparent electrical conductivity for (a) deep and (b) shallow data. All variograms were fitted with spherical models.

T a b l e 3. Variogram attributes ECa_d spherically fitted variogram models and ECa_s spherically fitted variogram models

	2009							2010	
	March	April	May	June	August	September	November	January	April
Deep apparent electrical conductivity (ECa_d)									
Nugget	0.07	0.03	0.08	0.04	0.05	0.06	0.05	0.01	0.03
Sill	1.06	1.16	0.98	0.90	1.02	1.02	1.15	0.91	1.30
Range	235.4	268.0	197.7	170.8	205.50	226.3	245.3	161.2	274.4
Shallow apparent electrical conductivity (ECa_s)									
Nugget	0.14	0.09	0.13	0.07	0.13	0.10	0.11	0.03	0.12
Sill	0.63	0.94	0.68	0.52	0.57	0.45	0.60	0.48	0.68
Range	218.3	333.90	245.0	106.8	160.70	170.5	181.2	119.7	220.0
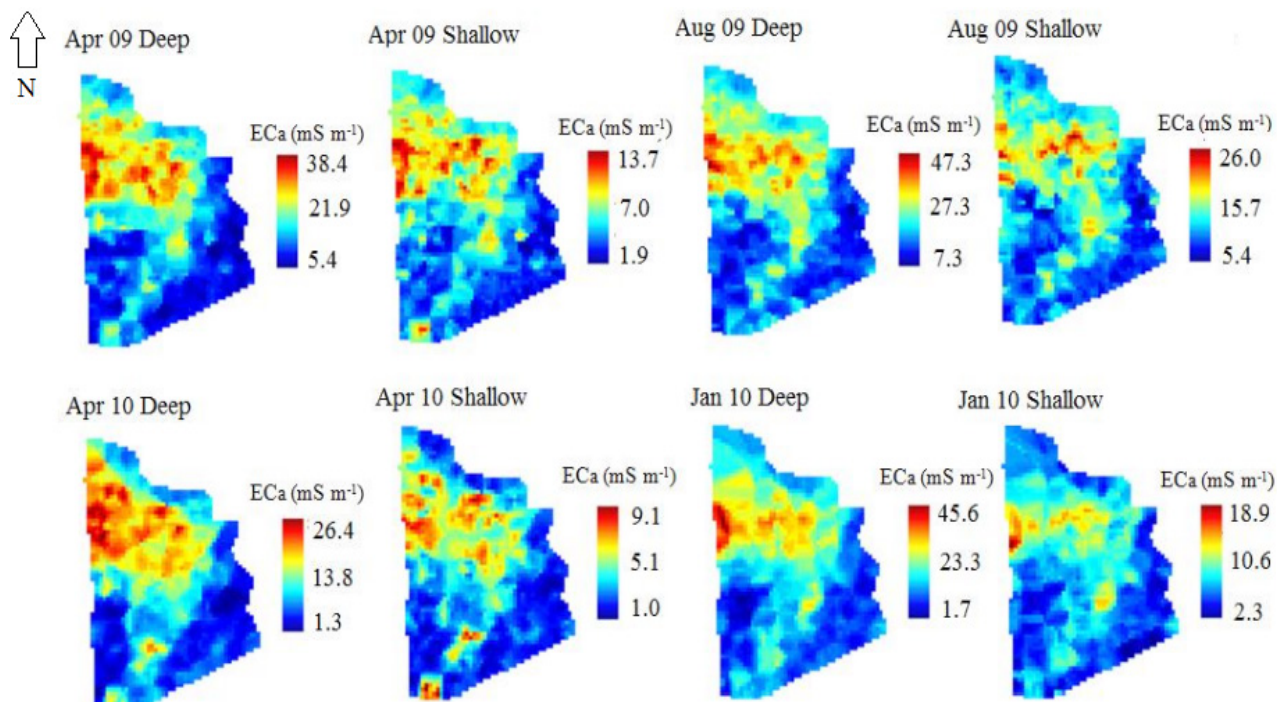
Fig. 5. Kriged apparent electrical conductivity (ECa) shallow and deep maps for selected months.

also redistributes soil sediments, by depositing the finest textured soil closer to the river basin, drains and depressions within the field. The standard deviation of the temporal stability map for the deep ECa measurements (Fig. 8) shows strong patterns. The locations of greatest change are associated with particular features of the field, such as a small shed along the eastern field boundary and a network of deep drains in the center of the field, where leached salts accumulated.

Both the shallow and deep ECa exhibited large-scale similarly stable temporal patterns, thus both ECa depths can be used to map the study site, however, since the feeder roots of cocoa is located in the ECa_s range, ECa_s would be better suited for soil management zone delineation. The results suggest that measurements of ECa patterns are independent of time and depth of measurement. Thus single ECa mapping should suffice for the delineation of stable management zones in cocoa fields.
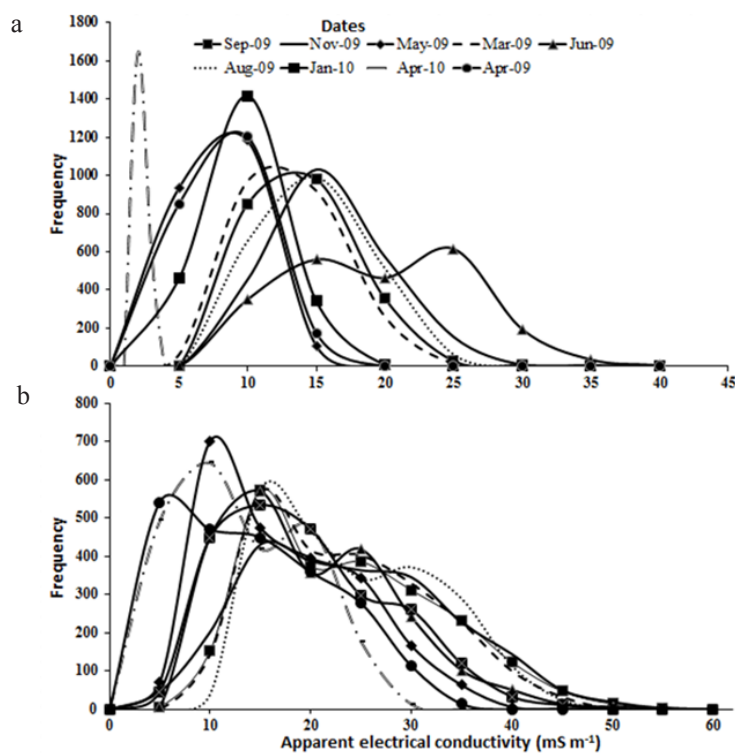
Fig. 6. Frequency distributions of kriged apparent electrical conductivity (ECa) for the study site: a – ECa deep distribution and b – ECa shallow distribution.

T a b l e 4. Descriptive statistics of soil properties

Variable	Mean	Median	Standard deviation	Minimum	Maximum	Coefficient of variance (%)
ECa_d (mS m^{-1})		17.8	5.2	1.2	35.0	29.2
ECa_s (mS m^{-1})	10.2	10.1	2.9	4.6	19.3	28.4
θ_g (g g^{-1})	0.28	0.28	0.10	0.18	0.42	35.7
Clay-silt (%)	79.1	77.5	24.5	40.0	113.4	31.0
pH	4.4	4.4	0.4	3.4	6.7	22.6
ECe (mS m^{-1})	126.4	123.1	34.1	60.0	283.2	27.0
Organic matter (%)	2.5	2.4	0.6	1.0	3.1	22.1

ECa_d – deep apparent electrical conductivity; ECa_s – shallow apparent electrical conductivity; θ_g – gravimetric water content; ECe – soil solution electrical conductivity.

CONCLUSIONS

1. Our results showed a positive linear dependence of both shallow apparent soil electrical conductivity and deep apparent soil electrical conductivity on clay-silt content and soil solution electrical conductivity. Thus, apparent soil electrical conductivity signals can be used to interpret clay-silt content, soil solution electrical conductivity and delineate management zones.

2. The significant correlations between apparent soil electrical conductivity and variables related to soil fertility such as organic matter, pH and gravimetric water content indicate that apparent soil electrical conductivity signals can also be used as soil fertility indicators.

3. Both the shallow apparent soil electrical con-ductivity and deep apparent soil electrical conducti-vity exhibited large-scale spatio-temporal pattern, thus both

T a b l e 5. Correlation matrix amongst soil properties in the study area

	ECa$_d$ (mS m^{-1})	ECa$_s$ (mS m^{-1})	θ_g (g g^{-1})	Clay-silt (%)	pH	ECe (mS m^{-1})
ECa$_d$ (mS m^{-1})	1					
ECa$_s$ (mS m^{-1})	0.690	1				
θ_g (g g^{-1})	0.278	0.250	1			
Clay-silt (%)	0.673	0.783	0.274	1		
pH	0.505	0.396	0.007	0.440	1	
ECe (mS m^{-1})	0.763	0.603	0.158	0.473	0.634	1
Organic matter (%)	0.201	0.232	0.330	0.221	0.175	0.094

Explanations as in Table 4.
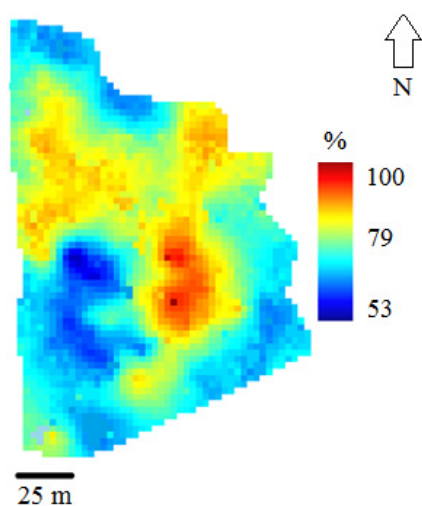
Fig. 7. Kriged spatial map of clay-silt % in the study site.

measurements would be suitable to delineate management zones in cocoa fields in the humid tropic. If fields are to be zoned based on the apparent soil electrical conductivity measurements, however, shallow apparent soil electrical conductivity would be preferable, since the feeding roots of cocoa trees are concentrated in the upper 0.2 m of the soil.

4. The multi-mapping strategy using electromagnetic induction provides useful information for delineating soil textural boundaries without the costly and time demanding soil sampling, instrument calibration and remapping.

5. For non-saline soils planted with perennial crops such as cocoa, the thick organic litter and understory cover coupled with humid tropical climate can minimize fluctuation in transient properties (soil water and temperature) resulting in apparent soil electrical conductivity signals that are time and depth independent.
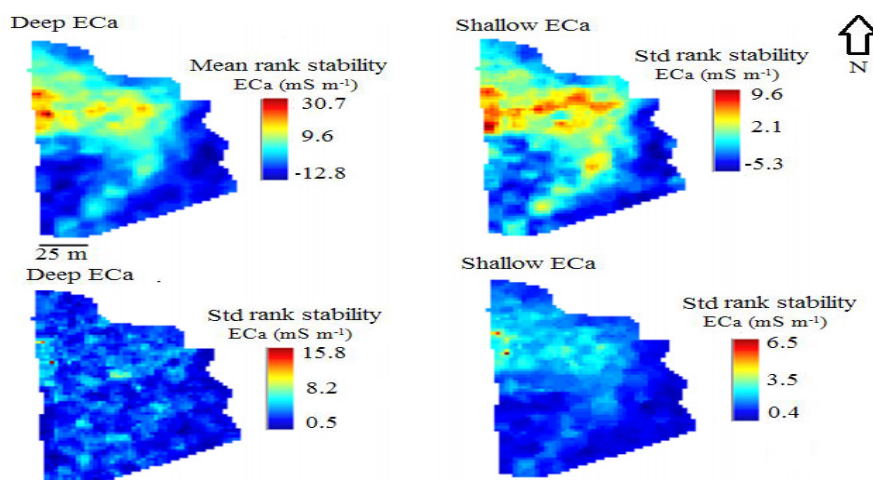

Fig. 8. Shallow and deep temporal stability maps of the nine apparent electrical conductivity (ECa) surveys. The light areas depict locations where the ECa is consistently higher than the field average, and the dark areas depict locations where the ECa is consistently lower than the field average. The light areas in the standard maps indicate the locations undergoing the most change. These locations are associated with a network of drains to the center of the field and a shed located along the eastern boundary.

6. One mapping is enough to determine underlying spatial patterns of properties related to soil fertility for efficient application of inputs and management of cocoa fields.

REFERENCES

Abdu H., Robinson D.A., and Jones S.B., 2007. Comparing bulk soil electrical conductivity determination using the DUALEM-1S and EM38-DD electromagnetic induction instruments. Soil Sci. Soc. Amer. J., 71, 189-196.

Atwell M., Wuddivira M., Gobin J., and Robinson D., 2013. Edaphic controls on sedge invasion in a tropical wetland assessed with electromagnetic induction. Soil Sci. Soc. Amer. J., 77, 1865-1874.

Bohling G., 2005. Introduction to geostatistics and variogram analysis. Available at: http://gismyanmar.org/geofocus/wp-content/uploads/2013/01/Variograms.pdf.

Bréchet L., Oatham M., Wuddivira M., and Robinson D.A., 2012. Determining spatial variation in soil properties in teak and native tropical forest plots using electromagnetic induction. Vadose Zone J., 11, DOI:10.2136/vzj2011.0102.

Burrough P.A. and McDonnell R.A., 1998. Principles of Geographical Information Systems. Oxford University Press, Oxford, UK.

Doerge T.A., 1999. Management zone concepts. Available at: http://www.ipni.net/publication/ssmg.nsf/0/C0D052F04A53E0BF852579E500761AE3/$FILE/SSMG-02.pdf.

Eneje R.C., Asawalam D.O., and Ezemobi C., 2012. Variability in physicochemical properties of some selected cocoa growing soils in Umuahia north local government area of Abia state. Res. J. Engr. Applied Sci., 1, 235-239.

Farahani H.J. and Buchleiter G.W., 2004. Temporal stability of soil electrical conductivity in irrigated sandy fields in Colorado. Trans. Amer. Soc. Agric. Eng., 47, 79-90.

Gockowski J., 2007. Cocoa production strategies and the conservation of globally significant rainforest remnants in Ghana. In: Production, markets, and the future of smallholders: the role of cocoa in Ghana. Inter. Inst. Trop. Agri., Accra, Ghana.

Goovaerts P., 2010. Geostatistical software. In: Handbook of applied spatial analysis. Springer Berlin Heidelberg, Germany.

Granger O.E., 1983. The hydroclimatology of a developing tropical island: a water resources perspective. Ann. Assoc. Amer. Geogra., 73, 183-205.

Haimelin R., 2008. Mapping soil water content on agricultural fields using electromagnetic induction. Report Helsinki Universty of Technology, Helsinki.

King J.A., Dampney P.M.R., Lark M., Mayr T.R., and Bradley R.I., 2001. Sensing soil spatial variability by electro-magnetic induction (EMI): its potential in precision farming. In: Third European Conference on Precision Agriculture (Eds G. Grenier, S. Blackmore), Montpellier, France.

Lesch S.M., Strauss D.J., and Rhoades J.D., 1995. Spatial prediction of soil salinity using electromagnetic induction techniques 1. Satistical prediction models: Acomparison of multiple linear regression and cokriging. Water Resour. Res., 31, 373-386.

Mann K.K., Schumann A.W., and Obreza T.A., 2011. Delineating productivity zones in a citrus grove using citrus production, tree growth and temporally stable soil data. Prec. Agri., 12, 457-472.

Martinez G., Vanderlinden K., Ordóñez R., and Muriel J.L., 2009. Can apparent electrical conductivity improve the spatial characterization of soil organic carbon? Vadose Zone J., 8, 586-593.

Moral F.J., Terrón J.M., and Silva J.R., 2010. Delineation of management zones using mobile measurements of soil apparent electrical conductivity and multivariate geostatistical techniques. Soil Till. Res., 106, 335-343.

Nehmdahl H. and Greve M.H., 2001. Using soil electrical conductivity measurements for delineating management zones on highly variable soils in Denmark. In: 3rd Eur. Conf. Precision Agriculture, Montpellier, France.

Obalum S.E., Oppong J., Igwe C.A., Watanabe Y., and Obi M.E., 2013. Spatial variability of uncultivated soils in derived savanna. Int. Agrophys., 27, 57-67.

Remy N., 2005. S-GeMS: The Stanford Geostatistical Modeling Software: A Tool for New Algorithms Development. In: Geostatistics Banff 2004: 7th Int. Geostatistics Conf., Quantitative Geology and Geostatistics, September 26 - October 1, Alberta, Canada, Springer, the Netherlands.

Rhoades J.D. and Chanduvi F., 1999. Soil salinity assessment: Methods and interpretation of electrical conductivity measurements. FAO, 57, 1-150.

Robinson D.A., Lebron I., Kocar B., Phan K., Sampson M., Crook N., and Fendorf S., 2009. Time-lapse geophysical imaging of soil moisture dynamics in tropical deltaic soils: An aid to interpreting hydrological and geochemical processes. Water Resour. Res., 45, DOI: 2008WR006984.

Rossi R., Amato M., Bitella G., and Bochicchio R., 2013. Electrical resistivity tomography to delineate greenhouse soil variability. Int. Agrophys., 27, 211-218

Schumann A.W., Fares A., Alva A.K., and Paramasivam S., 2003. Response of 'Hamlin' orange to fertilizer source, rate and irrigated area. In: Proceedings of Florida State Horticultural Society, 116, 256-260.

Snoeck D., Abolo D., and Jagoret P., 2010. Temporal changes in VAM fungi in the cocoa agroforestry systems of central Cameroon. Agro. Sys., 78, 323-328.

Triantafilis J. and Lesch S.M., 2005. Mapping clay content variation using electromagnetic induction techniques. Comp. Elec. Agri., 46, 203-237.

Vachaud G., Passerat De Silans A., Balabanis P., and Vauclin M., 1985. Temporal stability of spatially measured soil water probability density function. Soil Sci. Soc. Amer. J., 49, 822-828.

Walter C., McBratney A.B., Douaoui A., and Minasny B., 2001. Spatial prediction of topsoil salinity in the Chelif Valley, Algeria, using local ordinary kriging with local variograms versus whole-area variogram. Aust. J. Soil Res., 39, 259-272.

Wood G.A.R. and Lass R.A., 1985. Cocoa. Longman Group Limited, London, UK.

Wuddivira M.N., Robinson D. A., Lebron I., Bréchet L., Atwell M., De Caires S., Oatham M., Jones S.B., Abdu H. Verma A.K., and Tuller M., 2012. Estimation of soil clay content from hygroscopic water content measurements. Soil Sci. Soc. Amer. J., 76, 1529-1535.